Journal of
Ship&Ocean
Technology
©DECEMBER 2006

SOTECH Vol. 10, No. 4, pp. 1 ~ 11, 2006

Hybrid RANS and Potential Based Numerical Simulation for Self-Propulsion Performances of the Practical Container Ship

Jin Kim[1], Kwang-Soo Kim[1], Gun-Do Kim[1], Il-Ryong Park[1] and Suak-Ho Van[1]

[1] Maritime and Ocean Engineering Research Institute, KORDI, Daejeon, Korea;
Corresponding Author: jkim@moeri.re.kr

Abstract

The finite volume based multi-block RANS code, WAVIS developed at MOERI is applied to the numerical self-propulsion test. WAVIS uses the cell-centered finite volume method for discretization of the governing equations. The realizable k-ε turbulence model with a wall function is employed for the turbulence closure. The free surface is captured with the two-phase level set method and body forces are used to model the effects of a propeller without resolving the detail blade flow. The propeller forces are obtained using an unsteady lifting surface method based on potential flow theory. The numerical procedure followed the self-propulsion model experiment based on the 1978 ITTC performance prediction method. The self-propulsion point is obtained iteratively through balancing the propeller thrust, the ship hull resistance and towing force that is correction for Reynolds number difference between the model and full scale. The unsteady lifting surface code is also iterated until the propeller induced velocity is converged in order to obtain the propeller force. The self-propulsion characteristics such as thrust deduction, wake fraction, propeller efficiency, and hull efficiency are compared with the experimental data of the practical container ship. The present paper shows that hybrid RANS and potential flow based numerical method is promising to predict the self-propulsion parameters of practical ships as a useful tool for the hull form and propeller design.

Keywords: multi-block RANS, WAVIS, two-phase level set method, lifting surface method, self-propulsion

1 Introduction

The efforts to predict the hydrodynamic performances around a ship have been made for a long time. It has been usually carried out by an experiment in the towing tank. The computational fluid dynamic (CFD) for ship hydrodynamics is matured over the last decade. CFD technique is now adopted as the routine design process of a ship by supporting the designers to develop and evaluate the ship hull forms.

Maritime and Ocean Engineering Research Institute (MOERI) of Korea have been making an endeavor to develop the reliable CFD tool for the prediction of ship hydrodynamic performance. The developed code named as WAVIS is now spread out to

many Korean ships yards and widely used for the evaluation of a practical ship hull forms. As a link to this effort, the experimental data for the flow around practical hull forms are obtained to validate the CFD code (Van et al. 1997, 1998a and b). These data are also adopted as the test cases for the Gothenburg 2000 Workshop (Larsson et al. 2000). However, the most data are focused on flows around a bare hull to predict the total resistance and nominal wake, although the hull forms are much more modernized than those of the previous workshops (Larsson et al 1991, Kodama 1994).

Continued recent CFD Tokyo workshop (Hino 2005) suggested self-propulsion case for KRISO container ship (KCS) as one of the main bench-marking test cases. NMRI, Japan (Fujisawa et al. 2000) provides the experimental data for self-propelled condition of KCS to update the previous experimental data (Van et al. 1998b). Only for groups including WAVIS participated in this test case. Lubke from Potsdam Model Basin (Hino 2005) showed the best results by using the commercial CFD package CFX5. It was carried out with the rotating propeller, considering the real geometry and yielding the unsteady interactions between ship and propeller. However, this method still requires too much computing time to be used in practical applications.

In the present study, WAVIS code is applied to the free surface flow with the Level-Set formulation and self-propulsion simulation with the body force propeller by interacting with the unsteady lifting surface method. Under the consideration of the industrial use, the realizable k-ε two-equation turbulence model with a wall function and the 2nd order accurate numerical scheme is used to reduce the computing time and all computations are performed in a LINUX pc cluster, which has total 24 node with a Intel Pentium IV 3.2 GHz processor for each node. The computed results show a good agreement in self-propulsion parameters and also local flow behind the propeller. The total computing time was within 10 hours for each RANS computation.

2 Computational methods

The simulations at present study are performed by means of a finite volume based RANS code (WAVIS), currently used at MOERI/KORDI for the computation of incompressible turbulent flows around ship hulls. The free surface is captured with the two-phase level set method and body forces are used to model the effects of a propeller without resolving the detail blade flow.

2.1 Governing equations

The governing equations for turbulent free surface flow in the present study are the Reynolds-Averaged Navier-Stokes (RANS) equations for momentum transport and the continuity equation for mass conservation. The RANS and the continuity equations are expressed in integral form for a control volume Ω with a surface boundary S.

$$\frac{d}{dt}\int_{\Omega}\rho u_i d\Omega + \int_S \rho u_i u_j dS = \int_S \tau_{ij} n_j dS + \int_{\Omega}\rho b_i d\Omega \tag{1}$$

$$\frac{d}{dt}\int_{\Omega}\rho d\Omega + \int_S \rho u_i n_i dS = 0 \tag{2}$$

where ρ is the fluid density, u_i=(u,v,w) are velocity components in the Cartesian coordinate system, n_i is the unit normal vector, τ_{ij} is the fluid stress tensor, and b_i is the body force vector. All the fluid variables are made dimensionless with respect to advancing speed of a ship U_o, the ship length L, and the fluid density ρ. The dimensionless parameters, the Reynolds number (Re) and the Froude number (Fn), are defined respectively as

$$\mathrm{Re} = \frac{\rho U_o L}{\mu}, \quad \mathrm{Fn} = \frac{U_o}{\sqrt{gL}} \tag{3}$$

Stress tensor τ_{ij} can be written using Boussinesq's isotropic eddy viscosity hypothesis as follows.

$$\tau_{ij} = \mu_e \left(\frac{\partial u_i}{\partial x_j} + \frac{\partial u_j}{\partial x_i} \right) - \left(\hat{p} + \rho \frac{2}{3} k \right) \delta_{ij} \tag{4}$$

Here, $\hat{p}$ is the piezometric pressure ($= p + z/Fn^2$), k is turbulent kinetic energy, δ_{ij} is the Kronecker delta function and μ_e is the effective viscosity, i.e., the sum of turbulent eddy viscosity (μ_t) and the fluid molecular kinematic viscosity (μ).

For the turbulence closure, the realizable k-ε model (Shih et al. 1995) is used with Launder and Spalding's wall function (Launder and Spalding 1974). The discretization of the governing equations is carried out by the finite volume methods. Convection terms are discretized using QUICK scheme of the third order, and central difference scheme is utilized for diffusion terms. To ensure divergence-free velocity field, the SIMPLEC method is employed. The details of the present numerical methods can be found in (Kim et al. 2002).

2.2 Level-set method

The free surface is captured with the Level-Set method (Sussman et al. 1997). In order to obtain an accurate free surface solution and stable convergence, the computations are executed with a proper fine grid refinement around the free surface and with an adoption of implicit discretization scheme for the Level-Set formulation. Level-set function $\phi(x_i,t)$ is introduced to define the region of air, water, and free surface.

$$\begin{aligned} &\phi(x_i,t) > 0, \text{ if } x_i \in \text{water} \\ &\phi(x_i,t) < 0, \text{ if } x_i \in \text{air} \\ &\phi(x_i,t) = 0, \text{ if } x_i \in \text{free surface} \end{aligned} \tag{5}$$

The density and viscosity can be expressed with the function of $\phi(x_i,t)$ as follows:

$$\begin{aligned} \rho(\phi) &= \rho_a + (\rho_w - \rho_a) H(\phi) \\ \mu(\phi) &= \mu_a + (\mu_w - \mu_a) H(\phi) \end{aligned} \tag{6}$$

where, (ρ_w, μ_w) and (ρ_a, μ_a) represent the density and viscosity for water and air respectively. $H(\phi)$ is the Heaviside function with the relations: $H(\phi > 0)$=1, $H(\phi < 0)$=0, and $H(\phi = 0)$=0.5. In order to improve numerical smearing effects, the reinitialization step is

performed every time step and ensures that the Level-set is a signed distance function away from the interface ($\phi = 0$) without changing the location of the zero level set.

2.3 Lifting surface method

Since the effective wake and the propeller loading depend on each other, the overall process must be iterative. The iterative processes consist of two components, the propeller solver (Lifting Surface Method) and the RANS solver. The iterative process can start with the propeller analysis using the nominal wake as inflow. Using the computed propeller loading, the body force representing the propeller in the RANS equations can be calculated. The RANS solver computes the total velocity using the body force found earlier. The effective wake can be computed by subtracting the propeller induced velocity from the total velocity field. Finally, the propeller solver uses the effective wake as the inflow to compute the updated propeller loading. The iterative process continues until convergence is reached. The Lifting surface method (Kerwin and Lee 1987) is utilized in the present study because this method requires much less computing time and thus is used more in practice. The body force distribution is calculated from the instantaneous blade circulation distribution suggested by Choi (2000).

3 Hull form and experimental condition

KRISO container ship carrying 3,600 TEU, designed by MOERI/KORDI, was named as KCS. Table 1 and Figure 1 provide the principal particulars and the hull forms of the KCS and the geometrical parameter of the test propeller (KP505) is given in Figure 2. For the towing tank test, a model ship of KLNG was made of wood with the scale ratio of 1/31.5994 and the corresponding model propeller diameter was 0.25 m. In the towing tank test, a model ship was towed at the speed of Froude's similarity law that the speed ratio of model and prototype is square root of the scale ratio. The corresponding Reynolds and Froude numbers of KCS model ship was shown in Table 1. The model ship was fixed at the towing carriage by using two clamping. All the measurements were carried out in the fixed condition, where neither trim nor sinkage was allowed.

Figure 1: The hull forms of KCS

Table 1: Principal particulars of KCS

KCS	Prototype	Model
Scale ratio	31.5994	
L_{pp} (m)	230.0	7.2786
B (m)	32.2	1.019
T (m)	10.8	0.3418
Wetted surf. area (w/o rudder) (m^2)	9424	9.4379
Speed (m/s)	12.2456	2.196
Froude No. (Fn)	0.26	
Reynolds No. (Re)	2.39×10^9	1.4×10^7

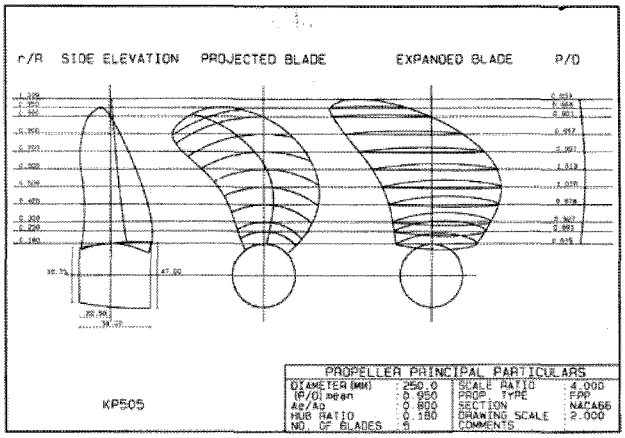

Figure 2: The propeller principal particulars for KP505

4 Computational results

4.1 Grid generations

The numerical results usually depend on the numerical schemes. However the generation of the proper numerical grid system is also very important to enhance the accuracy of numerical solution. Especially for the simulation of free surface flow, it is well known that the grid system on the free surface region has a great influence on the numerical results. The experience on simulating around the free surface flow leads to the proper grid arrangement including the free surface area with total 2,247,318 grid points, which is equivalent to the medium size grid in the previous study (Park et al. 2004). Starting from an IGES description of the KCS hull form, the commercial program GRIDGEN is used to generate H-O type multi-block grid system. Both starboard and port side are considered as a computational domain because of consideration on computing the self-propelled condition. Fig. 3 shows the grid system used in the present study.

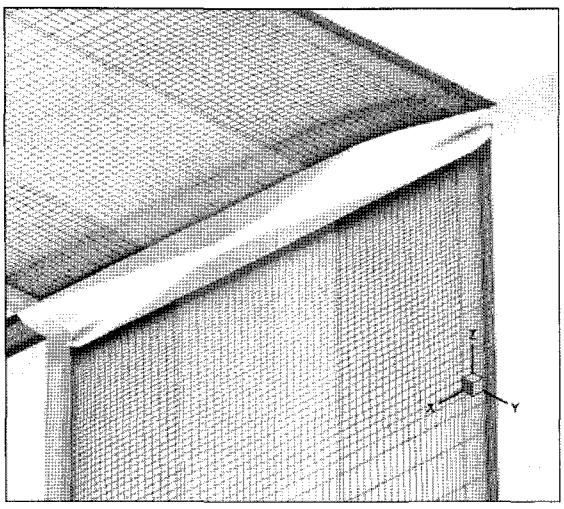

Figure 3: H-O Type total grid system for KCS hull form

4.2 Procedures and results for numerical self-propulsion test

The overall procedures for the numerical self-propulsion test are followed similar to real self-propulsion model test in towing tank.

4.2.1 Computation of the double body model flow without propeller

In order to compute the form factor (k), double model flow is computed. The form factor is obtained as recommended by CFDWS 2005 (Hino 2005).

$$1+k=(C_T)_{double-body}/C_{F0} \tag{7}$$

where $C_{F0}=\dfrac{0.075}{(\log_{10}\mathrm{Re}-2)^2}$, (ITTC 1957 frictional coefficient).

4.2.2 Computation of the free surface flow at towed condition without propeller

In order to obtain the total resistance and the nominal wake, the free surface flow at Fn = 0.26 is computed. Table 2 shows the comparisons of the resistance components such as the frictional resistance (C_F), the pressure resistance (C_P), the total resistance (C_T) coefficients, form factor ($1+k$) and nominal wake ($1-W_n$) respectively. The frictional resistance for the experiment is obtained from the ITTC-1957 line and the pressure resistance is the residuary resistance from the towing tank experiment. Therefore, it is not adequate to compare these components directly with the experiment. The computed total resistance coefficient shows about 1.1% error of the experimental data. The integrated nominal wake is 0.712 (ref. 0.686 in the experiment).

The comparison of the wave patterns and wave profile along the hull surface between the experiment and present result computed from the Level-Set formulation is shown in the Figure 4 and 5. The obtained wave patterns and hull surface wave profiles are in good agreement with the experiment. The prediction of wave patterns in the transom region is known as one of the difficult problems in the numerical simulation. The present study shows that the Level-Set formulation would be the robust numerical scheme in these kinds of problems. Figure 6 shows the comparisons of the computed axial velocity and cross flow vectors just downstream of the propeller, i.e., x/L_{PP}=0.4911. The computed results agree satisfactory with the experiment.

Table 2: The results of the numerical resistance test

Organization	Code	Resistance Coefficients ($\times 10^{-3}$)			$1+k$	$1-W_n$
		C_T(TOW)	C_P(TOW)	C_F(TOW)		
NMRI	Experiment	3.550		2.832*	1.100	0.686
MOERI	WAVIS	3.511	0.720	2.791	1.101	0.712
HSVA	COMET	3.526	0.863	2.663	1.072	0.745
SVA	CFX5	3.531	0.681	2.849	1.247	0.721
OPU	FLOWPACK	3.545	0.860	2.685	1.100**	0.634

* from ITTC 1957 friction line
** from experimental data

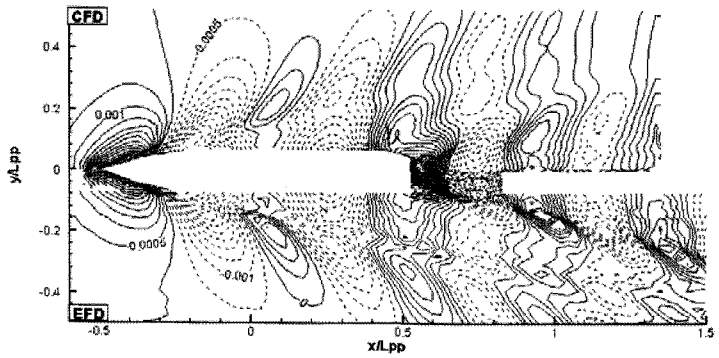

Figure 4: The comparison of wave patters around KCS hull form

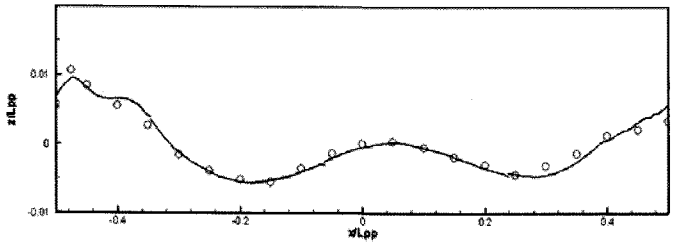

Figure 5: The comparison of wave profile along the KCS hull surface

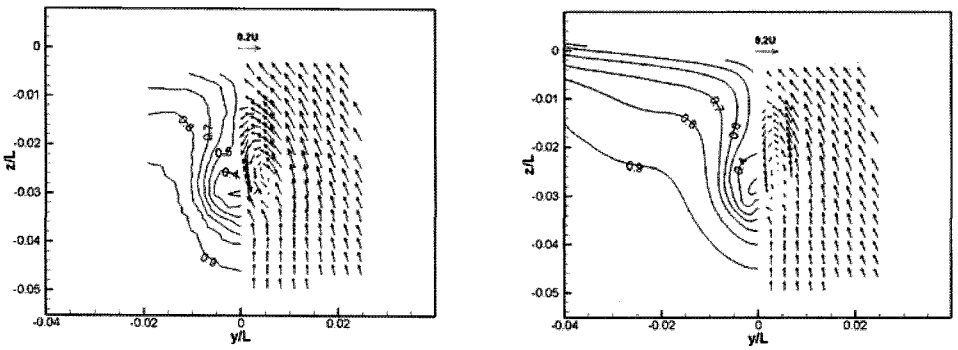

(a) Experiment (b) Computation

Figure 6: The comparison of the local velocity at x/LPP=0.4911

4.2.3 Computation of the self-propelled condition

Since the computation is performed at the model scale, the self-propulsion correction (*SFC*) is added to compensate the difference of the frictional coefficient between model and full scale, which is identically applied in the towing tank model test. The self-propulsion point is matched when the propeller thrust (T) is equal to the difference of the total resistance at self-propelled condition ($R_T(sp)$) and *SFC* as follows:

$$T = R_T(sp) - SFC \tag{8}$$

where $SFC = \{(1+k)(C_{F0M} - C_{F0S}) - \Delta C_F\} \times \frac{1}{2}\rho U^2 S_0$, $\Delta C_F = 0.27 \times 10^{-3}$, (Roughness allowance).

The iteration between RANS solver and propeller solver is performed until the self-propelled condition given in the equation (8) is satisfied. Table 3 shows the history of the convergence to find the self-propulsion state. The obtained self-propelled condition satisfies the order of 10^{-6} in the equation (8). In order to obtaine the self-propulsion parameters such as thrust deduction (t) and Taylor wake fraction (w_T), thrust identification method is applied to the computed propeller open water (POW) characteristics. Figure 7 shows the comparisons of POW characteristics between experiment and the lifting surface computation. After the thrust identification is performed at the computational POW lines (K_T=0.1706), the propeller efficiency (η_o), torque coefficient (K_{Qo}), and advance ratio (J_a) in POW condition is interpolated as shown in Figure 7. Table 4 gives the computed self-propulsion parameters and compared with other numerical method shown in CFDWS Tokyo (Hino 2005). Figure 8 and 9 shows the comparisons of the axial velocity and cross flow vectors at x/L_{PP}=0.4911 with propeller effect at self-propelled condition. The axial velocity contours just downstream of the propeller shown in Figure 8 agree well with the experiments. Because of the local difference of the cross plane vectors, which affect the local angles of attack into the propeller blade, the starboard part of the axial velocity is more accelerated than the port side.

Table 3: The history for finding self-propulsion condition

1st Iteration	Propeller Solver	rpm (n_1)	Advance ratio (J_{S1})	Thrust (K_{T1})	Torque (K_{Q1})
		8.7	1.009	0.1664	0.0272
	RANS Solver	C_T		(R_T-T-SFC) / $0.5\rho U^2 S_0$	
		3.823×10^{-3}		3.31×10^{-4}	
2nd Iteration	Propeller Solver	rpm (n_2)	Advance ratio (J_{S2})	Thrust (K_{T2})	Torque (K_{Q2})
		9.35	0.9395	0.1643	0.0308
	RANS Solver	C_T		(R_T-T-SFC) / $0.5\rho U^2 S_0$	
		3.903×10^{-3}		1.08×10^{-4}	
3rd Iteration	Propeller Solver	rpm (n_3)	Advance ratio (J_{S3})	Thrust (K_{T3})	Torque (K_{Q3})
		9.36	0.9385	0.1700	0.0287
	RANS Solver	C_T		(R_T-T-SFC) / $0.5\rho U^2 S_0$	
		3.908×10^{-3}		2.20×10^{-5}	
4th Iteration	Propeller Solver	rpm (n_4)	Advance ratio (J_{S4})	Thrust (K_{T4})	Torque (K_{Q4})
		9.38	0.9365	0.1706	0.0283
	RANS Solver	C_T		(R_T-T-SFC) / $0.5\rho U^2 S_0$	
		3.907×10^{-3}		1.10×10^{-6}	

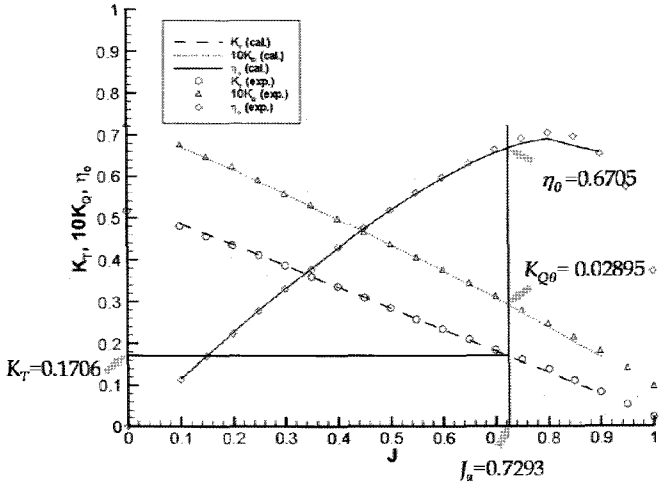

Figure 7: Thrust identification for self- propulsion parameters.

Table 4: Computed self-propulsion parameters

Organization	Code	1-t	1-w_T	η_o	η_r	J	n	η
NMRI	Experiment	0.835	0.792	0.682	1.011	0.728	9.50	0.740
MOERI	WAVIS	0.846	0.779	0.671	1.023	0.729	9.38	0.746
HSVA	COMET	0.865	0.789	0.667	0.981	0.725	9.56	0.717
SVA	CFX5	0.910	0.765	0.614	1.007	0.708	9.50	0.618
OPU	FLOWPACK	0.852	0.789	0.631	1.074	0.718	9.53	0.732

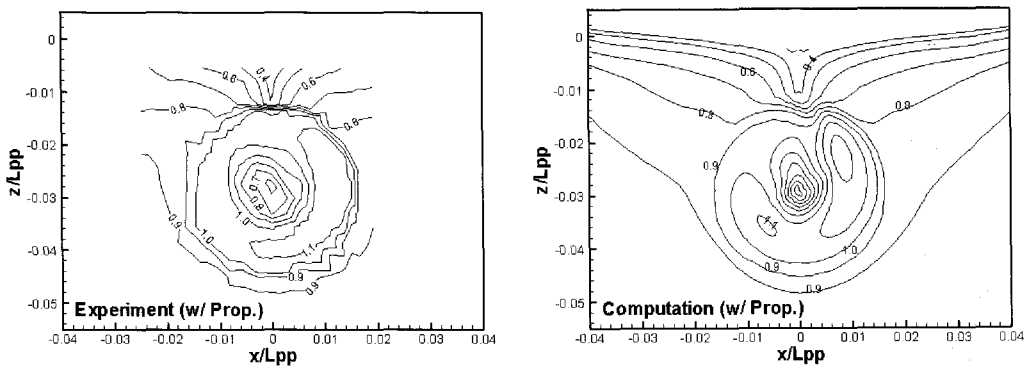

(a) Experiment (b) Computation

Figure 8: Axial velocity contours at x/L_{PP}=0.4911

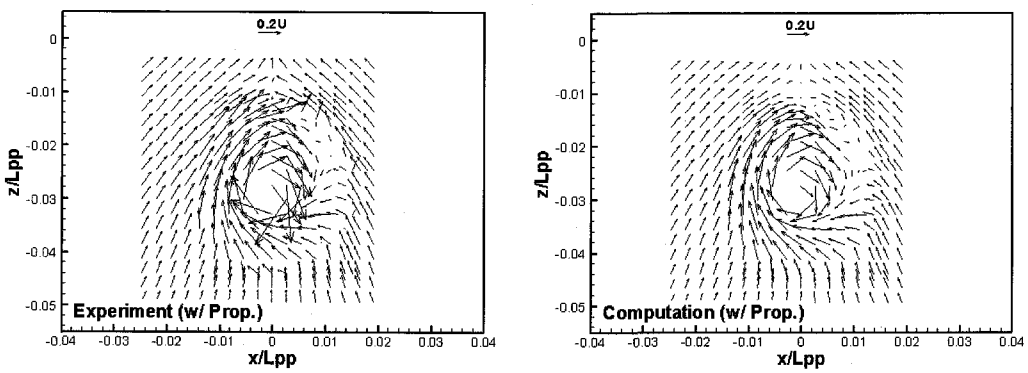

(a) Experiment (b) Computation

Figure 9: Cross flow vectors at x/L_{PP}= 0.4911

5 Conclusions

WAVIS code is updated and applied to numerical self-propulsion simulation for the KCS including free surface. The obtained results for the KCS show a great agreement with the experiment both in without and with a propeller case. The computed total resistance at towed condition gives the error of 1.1% C_T data. The self-propulsion point is obtained iteratively through balancing the propeller thrust, the ship hull resistance and towing force (SFC) that is correction for Reynolds number difference between the model and full scale. The self-propulsion parameters such as thrust deduction, wake fraction, propeller efficiency, and hull efficiency are quite good agreement with the experimental data of the KCS. The present paper shows that hybrid RANS and potential flow based numerical method is promising to predict the self-propulsion parameters of practical ships as a useful tool for the hull form and propeller design.

Acknowledgements

This research was sponsored by the Ministry of Commerce, Industry and Energy (MOCIE), Korea under the projects (PN00930) and also supported by the basic research project at MOERI/KORDI (PE0116C).

References

Choi, J.-K. 2000. Vortical Inflow-Propeller Interaction using an Unsteady Three-Dimensional Euler solver. Ph.D Thesis, Dept. of environmental and water resources engineering, Univ. of Texas, Austin, USA.

Fujisawa, J., Y. Ukon, K. Kume and H. Takeshi. 2000. Local Velocity Field Measurements around the KCS Model (SRI M.S.No.631) in the SRI 400m Towing Tank. Ship Performance Division Report No. 00-003-02, The Ship Research Institute of Japan.

Hino, T. 2005. Proc. of CFD Workshop Tokyo 2005, Tokyo, Japan.

Kerwin, J.E. and C.-S. Lee. 1987. Prediction of steady and unsteady marine propeller performance by numerical lifting surface theory. Trans. SNAME 86.

Kim, W.J., D.H. Kim and S.-H. Van. 2002. Computational study on turbulent flows around modern tanker hull forms. International Journal for Numerical Methods in Fluids, **38, 4,** 377-406.

Kodama, Y. (ed) 1994. Proceeding of CFD Workshop, Tokyo, Japan.

Larsson, L., V.C. Patel and G. Dyne (ed) 1991. Ship viscous flow, Proceeding of 1990 SSPA-CTH-IIHR Workshop, Gothenburg, Sweden.

Larsson, L., F. Stern and V. Bertram (ed) 2000. Gothenburg 2000: A Workshop on Numerical Ship Hydrodynamics, Gothenburg, Sweden.

Launder, B.E. and D.B. Spalding. 1974. The numerical computation of turbulent flows. Computer Methods in Applied Mechanics and Engineering, **3,** 269-289.

Park, I.-R., J. Kim and S.H. Van. 2004. Analysis of resistance performance of modern commercial ship hull form using a Level-Set method. Journal of the Society of Naval Architects of Korea, **41, 2,** 79-89 (in Korean).

Shih, T.-H., W.W. Liou, A. Shabir and J. Zhu. 1995. A new eddy viscosity model for high Reynolds number turbulent flows – model development and validation. Computers and Fluids, **24,** 227-238.

Sussman, M., E. Fatemi, P. Smerera and S. Osher. 1997. An improved Level-Set method for incompressible two-phase flows. Computers and Fluids, **27, 5-6,** 663-680.

Van, S.H., G.T. Yim, W.J. Kim, D.H. Kim, H.S. Yoon and J.Y. Eom. 1997. Measurement of flows around a 3600TEU container ship model. Proc. of the Annual Autumn Meeting, SNAK, Seoul, Korea, 300-304 (in Korean).

Van, S.H., W.J. Kim, D.H. Kim, G.T. Yim, C.J. Lee and J.Y. Eom. 1998a. Flow measurement around a 300K VLCC model. Proc. of the Annual Spring Meeting, SNAK, Ulsan, Korea, 185-188 (in Korean).

Van, S.H., W.J. Kim, G.T. Yim, D.H. Kim and C. J. Lee. 1998b. Experimental investigation of the flow characteristics around practical hull forms. Proc. of the 3rd Osaka Colloquium on Advanced CFD Applications to Ship Flow and Hull Form Design, Osaka, Japan.